JOURNAL OF SOLID STATE CHEMISTRY 115, 1–6 (1995)

The Layered Manganocuprate $Eu_3Ba_2Mn_2Cu_2O_{12}$: An Intergrowth between the "123" and "0201" Structures

M. Hervieu, C. Michel, R. Genouel, A. Maignan, and B. Raveau

Laboratoire CRISMAT, CNRS URA 1318-ISMRA, Université de Caen, Boulevard du Maréchal Juin, 14050 Caen Cedex, France

Received January 27, 1994; in revised form May 26, 1994; accepted June 6, 1994

A manganocuprate $Eu_3Ba_2Mn_2Cu_2O_{12}$ with a "0234" layered structure has been synthesized for the first time. This new phase crystallizes in the space group *I4/mmm* (a = 3.8826(1) Å, c = 35.266(1) Å). Its study by HREM and powder XRD shows that its structure consists of an intergrowth of single rock-salt layers with quadruple oxygen deficient perovskite layers. This structure can also be described as an intergrowth of K_2NiF_4-type layers, Eu_2MnO_4, with oxidized "123" layers $EuBa_2Cu_2MnO_8$. The semiconducting properties and paramagnetic behaviour of this phase at temperatures above 130 K suggest a mixed valence of manganese according to the formula $Eu_3^{III}Ba_2Mn^{III}Mn^{IV}Cu_2^{II}O_{12}$. An original feature of this compound deals with the existence of two magnetic orderings at 100 and 15 K respectively.

INTRODUCTION

The great flexibility of copper, due to its Jahn–Teller effect, has allowed numerous oxygen deficient intergrowths derived from the perovskite structure to be synthesized. Most of these cuprates are superconductors. Many investigations have been carried out on the substitution of different elements for copper in order to understand the relationships between superconductivity, magnetism, structure, and chemical bonding in these new materials. This is, for instance, the case for the "123" structure in which Cu(1) located between the pyramidal copper layers can be entirely replaced by niobium, tantalum, or titanium, changing the oxygen stoichiometry (1–3), or can be replaced by gallium or iron (4–6). Manganese, owing to its ability to exhibit oxidation states Mn(III) and Mn(IV) is an interesting candidate since it may also introduce particular magnetic properties. Although manganese perovskites are well known (7–12), as are the intergrowths $Sr_{n+1}Mn_nO_{3n+1}$ (13) and $Bi_2Sr_2MnO_{6+\delta}$ (14), no manganocuprate with such a layered structure has been evidenced as yet. We report on a new compound $Eu_3Ba_2Mn_2Cu_2O_{12}$ whose layered structure is based on an ordered distribution of copper and manganese and consists of a regular intergrowth of rock salt and oxygen-deficient perovskite layers.

CHEMICAL SYNTHESIS AND PRELIMINARY STRUCTURAL CHARACTERIZATION

After a preliminary exploration of the system Eu–Ba–Mn–Cu–O, our efforts were focused on the synthesis of the oxide corresponding to the formula $Eu_3Ba_2Mn_2Cu_2O_{12-\delta}$. This phase was prepared from an intimate mixture of Eu_2O_3, $BaCO_3$, MnO_2, and CuO heated at 1100°C in a platinum crucible for 4 hr in air. The sample was then reground and reheated in an oxygen flow at this temperature several times in order to obtain a single phase.

The X-ray powder diffraction pattern (Fig. 1), collected with a Philips vertical diffractometer, for the Cu$K\alpha$ radiation, in the range $10° \leq 2\theta \leq 80°$ at an increment of 0.02° (2θ), can be indexed in a tetragonal cell with a = 3.8826(1) Å and c = 35.266(1) Å.

The electron diffraction study, performed with a JEOL 200 CX electron microscope equipped with a eucentric goniometer (±60°), confirms this tetragonal cell with the reflection conditions $h\ k\ l$, $h + k + l = 2n$ (Fig. 2).

The EDS analysis performed with a KEVEX analyzer, shows that the composition does not vary from one crystal to the other and coincides with the nominal composition "$Eu_3Ba_2Cu_2Mn_2$."

STRUCTURE DETERMINATION: HREM AND XRD STUDY

In order to understand the layer stacking along the **c** axis, the crystals are first studied by high resolution electron microscopy (HREM). The [100] images are the most convenient for such a characterization. One of the images, in which the layer stacking can be easily identified on the basis of the contrast usually obtained for perovskite-based oxides, is shown in Fig. 3. The rows of bright dots are

0022-4596/95 $6.00

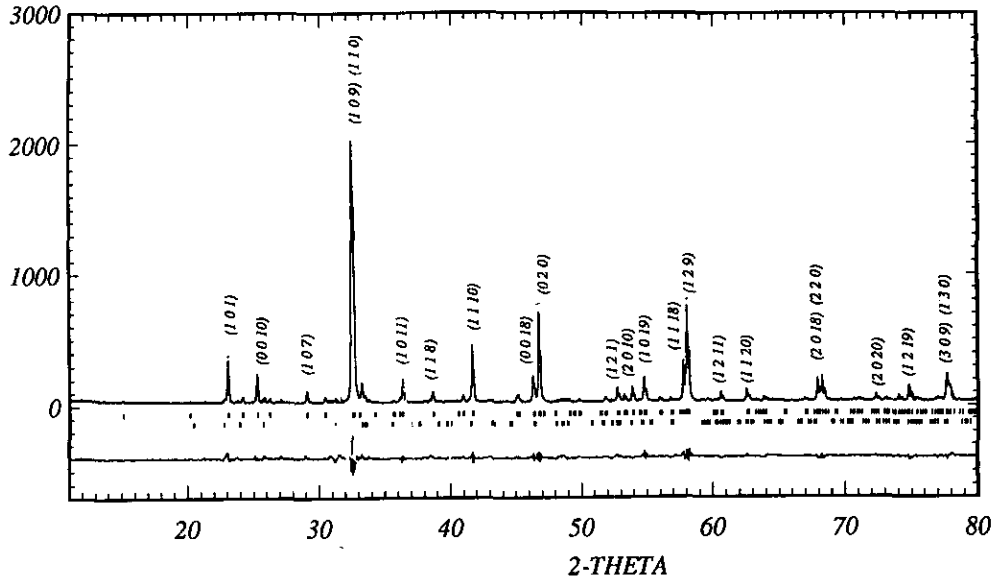

FIG. 1. Experimental (dotted line), calculated (solid line) X-ray diffraction pattern of $Eu_3Ba_2Cu_2Mn_2O_{12}$, with indices for some diffraction peaks. *Small bars indicate the Bragg angle positions for* $Eu_3Ba_2Cu_2Mn_2O_{12}$ *(upper bars) and* $EuMnO_3$ *(lower bars). At the bottom of the figure,* the difference X-ray pattern is plotted.

correlated to the $[CuO_2]_\infty$ and $[MnO_2]_\infty$ layers; it is of course impossible to differentiate Mn from Cu from these HREM images.

Along **c**, these rows of bright dots (B) are separated by double (R–R) and single (P) rows of gray dots and by a single row (F) of very weak dots according to the sequence

"B–R–R–B–P–B–F–B–P–B."

The two "R–R" rows of gray dots (small arrows) can be correlated to [EuO] rock-salt-type layers. The distance of 5.8 Å between the two surrounding bright rows (B) that correspond to $[Cu(Mn)O_2]_\infty$ layers supports this viewpoint.

The single (P) row of gray dots is similar to that observed for the $[BaO]_\infty$ layers of the "123" cuprate. The distance of 4.3 Å between the two bright rows that sandwich this layer agrees with that observed between two copper layers interleaved by a $[BaO]_\infty$ layer in the "123" structure.

The row of very weak dots (F) which involves a distance of 3.2 Å between the two surrounding $[CuO_2]_\infty$ layers exhibits a contrast similar to that observed for the $[Ln]_\infty$ layers of the "123" oxides. Thus it can be correlated to a $[Eu]_\infty$ layer, built up from europium ions located in fluorite cages between two pyramidal copper layers.

From these observations a model can be deduced corresponding to the following stacking of the different layers along **c**:

"$[MnO_2]$–[EuO]–[EuO]–$[MnO_2]$–[BaO]–$[CuO_2]$–[Eu]–$[CuO_2]$–[BaO]."

Thus this structural model (Fig. 4) consists of an intergrowth of rock-salt-type layers $[EuO]_\infty$ with a quadruple oxygen deficient perovskite layer, so that it can be described as an ordered "0234" oxide. Theoretical [100] images have been calculated for different focus values and crystal thicknesses, using positional parameters refined from XRD data (see below). They confirm the interpretation of the contrast. The calculated image corresponding to Fig. 3a is shown as example in Fig. 3b ($t \approx 31$ Å and $\Delta f \approx 0$ nm).

At this stage of the study, no proof of the ordering of manganese and copper has been given. Moreover, the nature of the $[EuO]_\infty$ layers, considered as rock salt layers, has to be confirmed since double fluorite-type layers cannot be discarded. The study of this structure from the X-

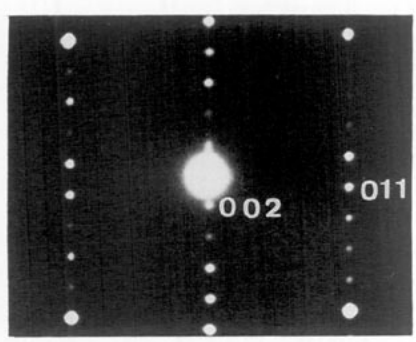

FIG. 2. $Eu_3Ba_2Cu_2Mn_2O_{12}$: (100)* electron diffraction pattern.

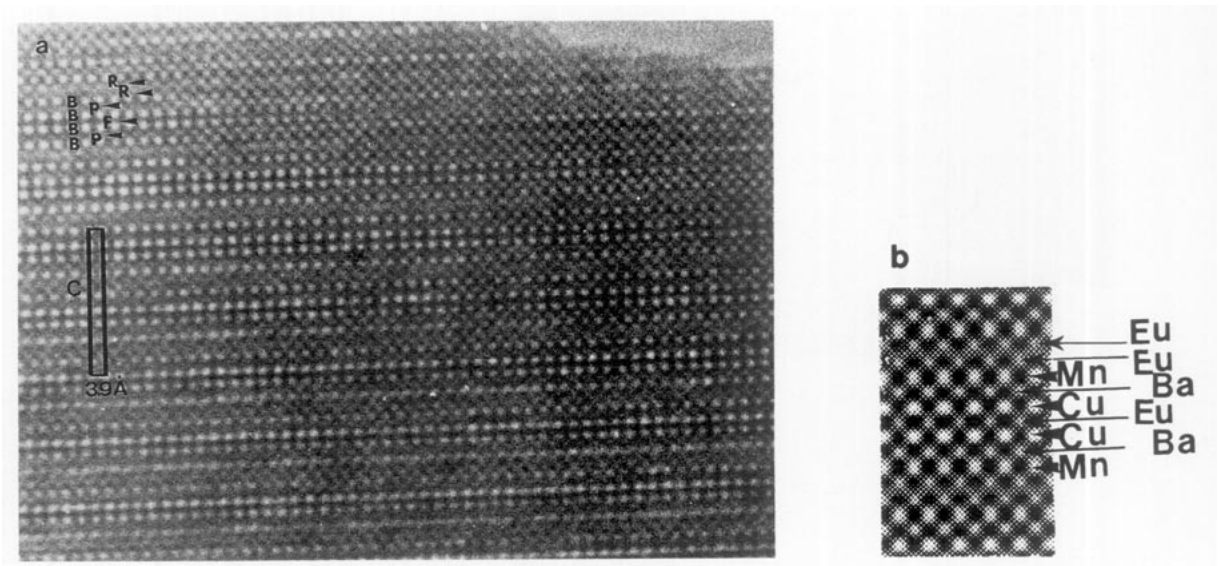

FIG. 3. (a) [100] HREM image showing the layer stacking along c. The different types of layers are identified: R, [EuO] rock salt-type layers; B, $[CuO_2]_\infty$ or $[MnO_2]$ layers; P, [BaO] layers; and *F*, [Eu] layers. (b) Corresponding calculated image.

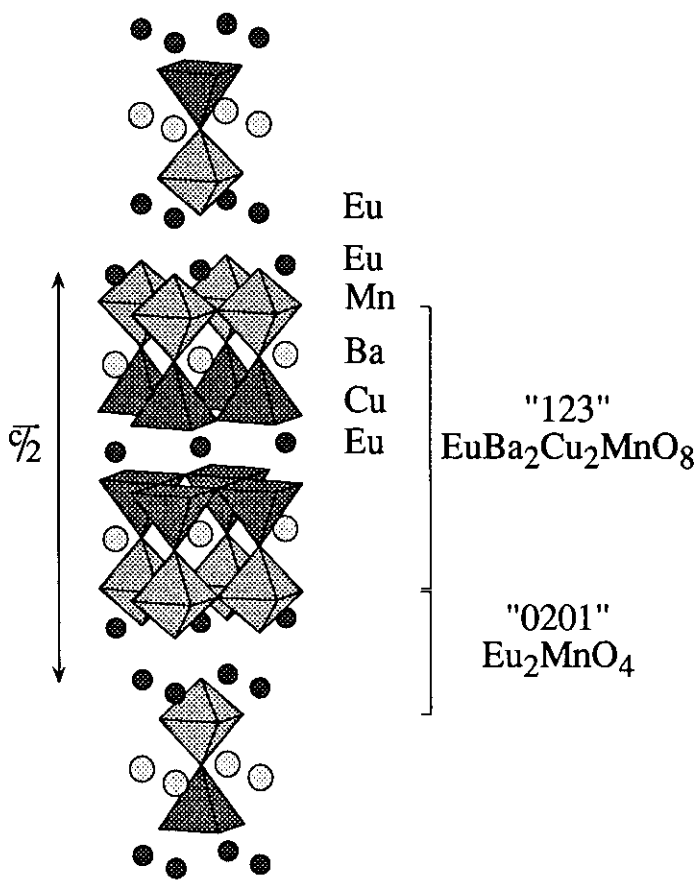

FIG. 4. Structural model corresponding to an ordered "0234" oxide for $Eu_3Ba_2Cu_2Mn_2O_{12}$.

ray powder diffraction data answers these questions. The calculations are performed in the space group *I4/mmm* using the profile analysis computer program DBW3.2 (15).

Starting from the above ideal model, the different ions are located in the 2*b*, 4*e*, and 8*g* sites of the corresponding space group (see Table 1). $EuMnO_3$ (16, 17) detected as an impurity is introduced as secondary phase. After refinement of the background parameters and then of the linewidth parameters, the different positional variables (*z*), and the isotropic thermal factors (*B*) are refined successively except for oxygen ions whose *B* factors are fixed at 1 Å^2. This allows the different *R* factors to be lowered to $R_p = 0.0794$, $R_{wp} = 0.111$, $R_i = 0.063$, and $\chi^2 = 2.15$ for the different variable values given in Table 1.

TABLE 1
Refined Parameters for $Eu_3Ba_2Mn_2Cu_2O_{12}$ (Space Group No. 139, *I4/mmm*); $a = 3.8826(1)$ Å, $c = 35.266(1)$ Å)

	Site	*x/a*	*y/b*	*z/c*	*B*(Å^2)
Eu(1)	2*b*	0	0	1/2	0.1(1)
Eu(2)	4*e*	0	0	0.7127(1)	1.1(1)
Ba	4*e*	0	0	0.6049(1)	0.1(1)
Cu	4*e*	0	0	0.0470(2)	0.5(1)
Mn	4*e*	0	0	0.1664(2)	0.5(1)
O(1)	8*g*	1/2	0	0.0409(5)	1[a]
O(2)	4*e*	0	0	0.1144(7)	1[a]
O(3)	8*g*	1/2	0	0.1732(5)	1[a]
O(4)	4*e*	0	0	0.220(1)	1[a]

Note. $R_p = 0.0794$, $R_{wp} = 0.111$, $R_i = 0.063$ $\chi^2 = 2.15$.
[a] Not refined.

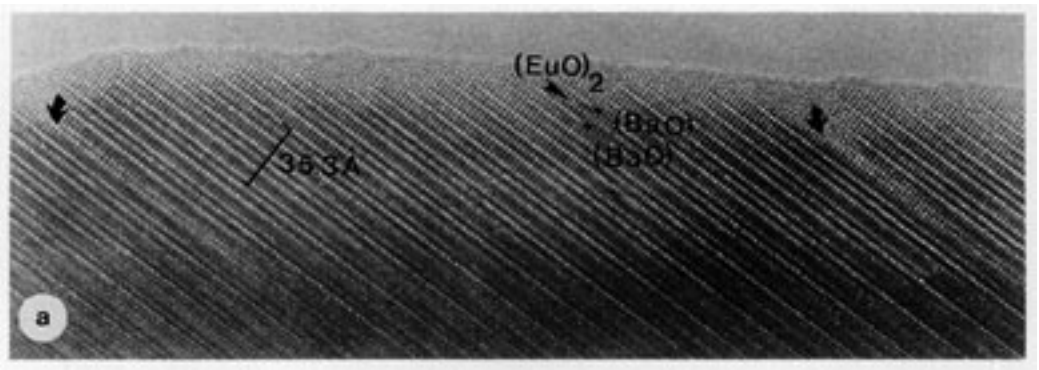

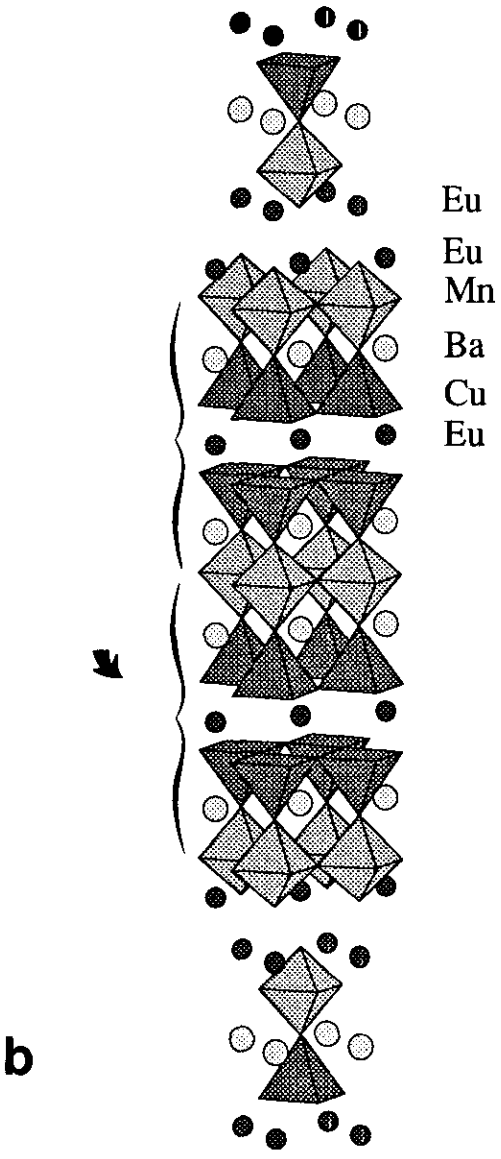

FIG. 5. (a) HREM image of localized defects (curved arrows) corresponding to the appearance of "123" extra slices. (b) (Eu_2MnO_4) $(EuBa_2Cu_2Mn_2O_8)_2$: idealized drawing of the structure resulting from the addition of a "123" slice.

TABLE 2
Selected Interatomic Distances (Å)

Eu(1)–O(1)	×8 2.42(1)	Cu–O(1)	×4 1.953(2)
Eu(2)–O(3)	×4 2.39(1)	Cu–O(2)	×1 2.38(2)
Eu(2)–O(4)	×4 2.757(3)	Mn–O(2)	×1 1.83(1)
Eu(2)–O(4)	×1 2.37(3)	Mn–O(3)	×4 1.956(2)
Ba–O(1)	×4 2.98(1)	Mn–O(4)	×1 1.89(4)
Ba–O(2)	×4 2.766(3)	Cu–Cu[a]	3.31(1)
Ba–O(3)	×4 3.09(1)	O(1)–O(1)[a]	2.88(2)

[a] Distances along **c**.

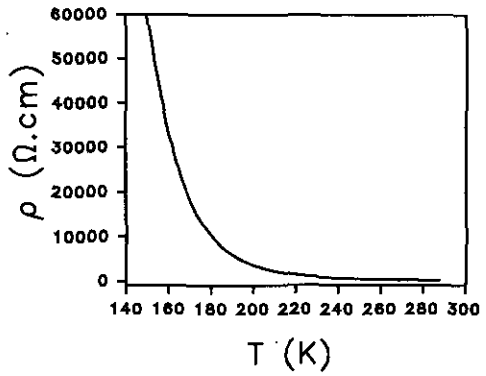

FIG. 6. Temperature dependence $e(T)$ of the resistivity for $Eu_3Ba_2Cu_2Mn_2O_{12}$.

At this stage other possibilities have to be tested. The first one deals with the fact that copper sits on the manganese sites and vice versa. Calculations involving copper on the octahedral sites and manganese in the pyramidal sites do not show any significant change in the R factor but lead to a significant increase of B(Cu), whereas B(Mn) becomes negative, so that this hypothesis can be definitely rejected. The second possibility that can be considered deals with the introduction of oxygen between the CuO_5 pyramids, in the $[Eu_{(1)}]_\infty$ plane in order to transform the CuO_5 pyramids into CuO_6 octahedra. Calculations with this model lead to a significant increase in the R factors (especially of R_i): $R_p = 0.0856$, $R_{wp} = 0.119$, $R_i = 0.083$, and $\chi^2 = 2.47$, and can also be rejected in agreement with the too short Cu–Cu distances along **c** (Table 2), and the chemical analysis by redox titration which shows that the oxygen content is closed to 12.

Finally, the third possibility corresponds to a different arrangement of the oxygen atoms within the Eu(2) layers, leading to double fluorite-type layers. This hypothesis leads to a significant increase of the R factors is also observed ($R_p = 0.089$, $R_w = 0.123$, and $R_i = 0.097$) so that it must also be rejected.

The calculated interatomic distances (Table 2) are compatible with those usually observed in these kinds of oxides. Note, however that two Mn–O distances are rather short, ranging from 1.83 to 1.89 Å. Such Mn–O bonds, shorter than 1.9 Å, have already been observed in several manganese oxides such as α-Mn_2O_3 (18), MnO_2 (19), $LiMnO_2$ (20), and $BaMnO_3$ (21).

This structural study definitely establishes that a new intergrowth, characterized by the "0234" structure has been synthesized. The analysis of this structure shows that it can be described (Fig. 4) as an intergrowth of two well-known structural types, the "0201," i.e., the K_2NiF_4-type structure that corresponds here to Eu_2MnO_4 slices, and the oxidized "123" structure that corresponds here to $EuBa_2Cu_2MnO_8$ slabs, according to the formula $(Eu_2MnO_4)_n(EuBa_2Cu_2MnO_8)_{n'}$.

It is worth pointing out that the stacking of the "0201" and "123" layers is regular. Only some intergrowth defects are sometimes observed as shown in Fig. 5a (curved arrows). In this [110] image, the barium and europium layers are highlighted; at the level of the defect, it appears that one $[MnO_2]$ and two (EuO) layers have disappeared, leading to the local formation of an additional "123" slice that may correspond to the member $n = 1$, $n' = 2$, i.e., to the formula $(Eu_2MnO_4)(EuBa_2Cu_2Mn_2O_8)_2$.

ELECTRIC AND MAGNETIC PROPERTIES

The electrical resistivity measured versus temperature in the range 130–300 K, with the four probe method shows a semiconducting behavior (Fig. 6). A resistivity of 100 Ω cm is indeed observed at room temperature, and resistivity increases as T decreases. The plot of $\ln(R/R_0) = f(10^3/T)$ (Fig. 7) evidences an activation energy of 0.17 eV. These results show that the charge carriers are localized.

The magnetic susceptibility measured in the range 4–600 K (Fig. 8) shows that two magnetic orderings appear at 100 and 15 K respectively. Note that the second ordering is probably ferromagnetic since for $T < 15$ K a hysteresis cycle is observed (Fig. 9). Such magnetic

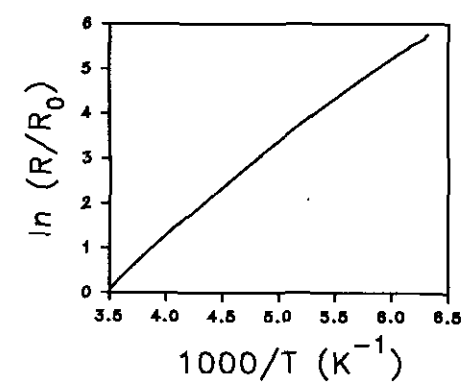

FIG. 7. T^{-1} dependence of $\ln(R/R_0)$. The activation energy has been calculated from the slope of this plot.

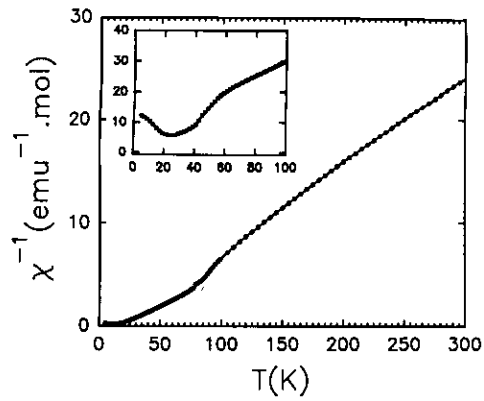

FIG. 8. Temperature dependence $\chi^{-1}(T)$ of the inverse of the magnetic susceptibility for $Eu_3Ba_2Cu_2Mn_2O_{12}$ registered with an applied field of 0.3 T. Inset also shows the $\chi^{-1}(T)$ curve for $EuMnO_3$.

orderings can be considered as characteristic of the present phase and are not due to impurities. Note indeed that the magnetic ordering of $EuMnO_3$ that appears as an impurity in the present preparation takes place at a different temperature (Fig. 8). The experimental effective magnetic moment deduced from the slope of the curves $\chi^{-1} = f(T)$ of the paramagnetic domain is higher than those calculated for the two possible mixed valent formulae, $Eu_3^{III}Ba_2^{II}Mn^{III}Mn^{IV}Cu_2^{II}O_{12}$ and $Eu_3^{III}Ba_2^{II}Mn_2^{III}Cu^{II}Cu^{III}O_{12}$, using the following moments (22) of 3.4 μ_B for Eu^{3+}, 5.1 μ_B for Mn^{3+}, 4 μ_B for Mn^{4+}, 2.2 μ_B for $Cu2^+$, and 0 μ_B for Cu^{3+}; one indeed obtains calculated values of 9.3 μ_B and 9.5 μ_B for these two formulas respectively, for an experimental value of 9.8 μ_B. Thus it is not possible to decide between these two possibilities from the value of the magnetic moment. Nevertheless, the low value of the conductivity suggests that the mixed valence Cu(II)–Cu(III) does not exist in this phase, so that the mixed valence Mn(III)–Mn(IV) corresponds to the most reasonable configuration.

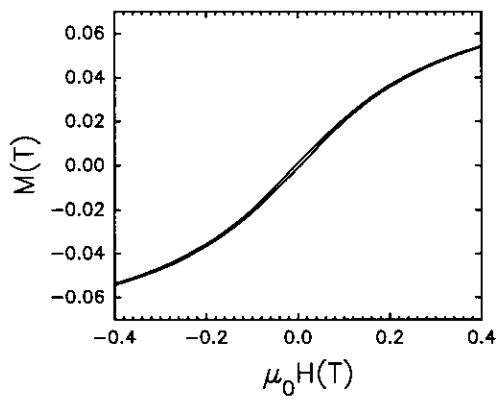

FIG. 9. Magnetic field dependence $M(H)$ of the magnetization registered at 5 K.

CONCLUDING REMARKS

A new manganocuprate $Eu_3Ba_2Mn_2Cu_2O_{12}$, with an original "0234" structure has been synthesized. This oxide that is characterized by an ordered distribution of the manganese and copper ions, represents the first member ($n = n' = 1$) of a series of intergrowth with the generic formula $(Eu_2MnO_4)_n(EuBa_2Cu_2MnO_8)_{n'}$ whose investigation is in progress. A neutron diffraction study will be performed in order to understand the original magnetic properties of this new phase.

REFERENCES

1. N. Muroyama, E. Sudo, K. Kani, A. Tsuzuki, S. Kawakami, M. Awano, and Y. Torii, *Jpn. J. Appl. Phys.* **27,** L1623 (1988).
2. C. Greaves and P. R. Slater, *Physica C* **161,** 245 (1989).
3. M. J. Rey, P. Dehaudt, J. Joubert, and A. W. Hewat, *Physica C* **167,** 162 (1990).
4. G. Roth, P. Adelmann, G. Heger, R. Knitter, and Th. Wolf, *J. Phys. I* **1,** 721 (1991).
5. J. T. Vaughey, J. P. Thiel, E. F. Hasty, D. A. Groenke, C. L. Stern, K. R. Poeppelmeier, B. Dabrowski, D. G. Hinks, and A. W. Mitchell, *Chem. Mater.* **3,** 935 (1991).
6. P. Garcia Gonzales, Doctoral Thesis, Madrid, 1992.
7. H. L. Yakel, *Acta. Crystallogr.* **8,** 394 (1955).
8. G. H. Jonker and J. H. Van Santen, *Physica C* **16,** 337 (1980).
9. V. Caignaert, N. Nguyen, M. Hervieu, and B. Raveau, *Mater. Res. Bull.* **20,** 479 (1985).
10. A. Reller, J. M. Thomas, D. A. Jefferson, and M. K. Uppal, *Proc. R. Soc. London A* **394,** 223 (1984).
11. V. Caignaert, M. Hervieu, N. Nguyen, and B. Raveau, *J. Solid State Chem.* **62,** 281 (1986).
12. K. R. Poeppelmeier, M. E. Leonowicz, J. C. Scanlon, J. M. Longo, and W. B. Yelon, *J. Solid State Chem.* **45,** 71 (1982).
13. Mizutani, *J. Chem. Soc. Ind.* **73,** 1097 (1970).
14. J. M. Tarascon, Y. Le Page, W. R. McKinnon, R. Ramesh, M. Eibshutz, E. Tselepis, E. Wang, and G. W. Hull, *Physica C* **167,** 20 (1990).
15. D. B. Wiles and R. A. Young, *J. Appl. Crystallogr.* **14,** 149 (1981).
16. S. Quezel-Ambrunaz, *Bull. Soc. Fr. Mineral. Cristallogr.* **91,** 339 (1968).
17. G. J. McCarthy, P. V. Gallagher, and C. Sipe, *Mater. Res. Bull.* **8,** 1277 (1973).
18. S. Geller, *Acta Crystallogr. B* **27,** 821 (1971).
19. W. H. Baur, *Acta Crystallogr. B* **32,** 2200 (1976).
20. G. Dittrich and R. Hoppe, *Z. Anorg. Allg. Chem.* **368,** 262 (1969).
21. A. D. Potoff, B. L. Chamberland, and L. Katz, *J. Solid State Chem.* **8,** 234 (1973).
22. P. W. Selwood, "Magnetochemistry," p. 159. Interscience, New York, 1956.